Transport Properties of Saturated and Unsaturated Porous Fractal Materials

S. W. Coleman* and J. C. Vassilicos

Department of Aeronautics and Institute for Mathematical Sciences, Imperial College, London, SW7 2BY, United Kingdom

(Received 29 August 2007; published 24 January 2008)

Inviscid, irrotational flow through fractal porous materials is studied. The key parameter is the variation of tortuosity with the filling fraction ϕ of fluid in the porous material. Altering the filling fraction provides a way of probing the effect of the fractal structure over all its length scales. The variation of tortuosity with ϕ is found to follow a power law of the form $\alpha \sim \phi^{-\epsilon}$ for deterministic and stochastic fractals in two and three dimensions. A phenomenological argument for the scaling of tortuosity α with filling fraction ϕ is presented and is given by $\alpha \sim \phi^{D_w - 2/D_f - d_E}$, where D_f is the fractal dimension, D_w is the random walk dimension, and d_E is the Euclidean dimension. Numerically calculated values of the exponents show good agreement with those predicted from the phenomenological argument for both the saturated and the unsaturated model.

DOI: 10.1103/PhysRevLett.100.035504 PACS numbers: 61.43.Gt, 61.43.Hv, 66.30.−h

Porous materials such as aerogels [1], sedimentary rocks [2], and fracture systems [3] are now widely accepted to exhibit fractal characteristics. The multiscale geometry of these materials has been found to have a significant effect on their transport properties. For example, the permeability of a fracture is substantially increased if the fracture interface has fractal characteristics [4]. The characterization of porous materials and their transport properties, such as permeability and thermal conductivity, has historically been limited to the measurement of macroscopic parameters, which tells one little about the mesoscopic structure of these materials. There has been much progress [5,6] in using microtomography images to generate 3D networks from which flow properties can be predicted. However it is not always easy to draw a relationship between observable transport properties and simple geometrical quantities. Furthermore, despite the advances mentioned, predictions of these properties is still largely based on empirical relationships based on observable characteristics of the geometry, such as porosity [7].

A common parameter used to describe this mesoscopic structure is the tortuosity α, which represents the tortuous or twisted nature that a fluid would have to take to pass through the porous material. Here, tortuosity is taken as a dimensionless quantity which quantifies the added mass effect caused by fluid flowing around an obstruction [8], $\alpha = \frac{\rho^*}{\rho_f}$, where $\rho*$ is the effective density and ρ_f is the bulk fluid density. Reference [9] described an experimental method of determining the tortuosity of 91% porous aerogel using a superfluid ^{4}He film of varying thickness. Thin films follow all the irregularities of the substrate, while thick films ''defractalize'' the substrate and only large scale features remain important. It was proposed that the scaling of tortuosity with the volume filling fraction ϕ of liquid helium could act as an independent fractal characteristic of the material. The exponent of this scaling $-\epsilon$ was found to be to be approximately -1.0 for the aerogel sample used in the experiment. This can be treated as the scaling of a dynamical property in a fractal environment.

This Letter aims to determine, both phenomenologically and numerically, the relationship between tortuosity and volume filling fraction in a wide class of saturated and unsaturated fractals, including a model for the aerogel used in this experiment.

There are several theories in the literature for the dependence of the tortuosity of random or fractal networks with increasing volume filling fraction of fluid, e.g., [10–12]. All of the theories share the feature that the scaling exponent is solely a function of the box-counting dimension D_f of the material, which describes how the mass M of a fractal scales with the length scale L being examined, $M \sim L^{d_E} n(L) \sim L^{D_f}$, where $n(L)$ is the density of the fractal and d_E the Euclidean dimension of the embedding space. Yet, it has long been known that the description of dynamic properties, such as diffusion on fractals, also requires the random walk dimension D_w [13]. The key result is that diffusion on a fractal is range dependent, so that the diffusion coefficient $D(L) \sim L^{2-D_w}$.

To obtain a scaling relationship for tortuosity, it must be related to diffusion. The equivalence between the hydrodynamical problem of an inviscid, incompressible fluid flowing in a pore space and that of the electrical conductivity σ of a nonconducting, rigid porous material, containing a conducting pore fluid of conductivity σ_f allows the tortuosity to be expressed as [8,14]

$$\alpha = \frac{\sigma_f}{\sigma}\phi. \tag{1}$$

The final step needed is a relationship between conductivity and diffusion, which is provided by the famous Einstein equation [15] $D = k_B T\theta$, where k_B is Boltzmann's constant, T is the temperature and θ is mobility. Ohm's Law gives $\sigma = qn\theta$, where n is the concentration of current carrying particles and q their charge. This has been shown to hold in the case of inhomogeneous networks [16]. Thus,

the diffusion coefficient is given by

$$D(L) = \frac{k_B T \sigma(L)}{q n(L)} \sim \frac{\sigma(L)}{n(L)}. \quad (2)$$

Assuming that the adsorbed film is relatively thin and using the scalings observed for fractals for $D(L)$ and $n(L)$, it is easy to show that $\sigma(L) \sim L^{D_f - D_w + 2 - d_E}$. Noting that $\phi \sim L^{D_f - d_E}$ [10] and substituting this expression in Eq. (1), the following scaling between tortuosity and filling fraction is obtained,

$$\alpha \sim \phi^{D_w - 2/D_f - d_E}. \quad (3)$$

This implies that the scaling of tortuosity with filling fraction is determined by the box-counting and random walk dimensions of the fluid. Of course, for small filling fractions, these fractal dimensions are closely related to the fractal dimensions of the adsorbant, with the further assumption that there are no correlations between layers on different surfaces. Thus, knowledge of this scaling enables one to determine the fractal characteristics of the adsorbant.

Two approaches are taken to model the problem at hand. The first is to consider a saturated pore space with a fractal mass distribution given by a deterministic fractal, where in this case the families of 2D Sierpinski carpets and 3D Menger sponges (see [17]) were considered. The defractalization is achieved by considering different generations of the fractal, rather than by increasing the filling fraction of fluid in the unsaturated pore, as in [9]. As the number of iterations is decreased, more of the small scale features of the fractal are lost and it can be imagined that this resembles the smoothing out of small scale features by a thicker adsorbed film. There is no attempt to model the dynamics of the filling and draining process in this approach, rather it is intended to reflect the defractalization of the fractal object by increased filling fraction. The incompressibility and irrotationality associated with superfluid ^{4}He (see [9]) lead to a boundary value problem in the field of potential flow, with the scalar velocity potential ψ. The velocity field $\boldsymbol{v}$ is given by $\nabla\psi = \boldsymbol{v}$.

The porous medium occupies the space $0 < x < L$, where L is large compared to the size of the pores, and has a total lateral area A. A potential difference ψ_L is applied across the porous medium and zero-flux boundary conditions are enforced on all other boundaries. The filling fraction ϕ is defined by considering the function $\gamma(\boldsymbol{r})$ which is 0 when $\boldsymbol{r}$ is occupied by the porous material and 1 when it is occupied by fluid. Clearly, $\phi = \frac{1}{LA} \int \gamma(\boldsymbol{r}) d^3\boldsymbol{r}$. The tortuosity given in [8] can be extended to the case of unsaturated media by taking the ratio of the kinetic energy of the tortuous flow to the kinetic energy of a flow with no obstruction to give

$$\alpha = \frac{\phi A (\psi_L)^2}{L \int \gamma(\boldsymbol{r}) (\nabla\psi)^2 d^3\boldsymbol{r}}, \quad (4)$$

or its equivalent 2D definition. The potential equations are solved using a simple linear finite element scheme [18]. Figure 1 shows typical results for the variation of tortuosity α with filling fraction ϕ, in this case for flow around a 2D Sierpinski gasket with $D_f = 1.87$ and $D_w = 2.13$, where the fluid flow takes place in the fractal part of the gasket. Clearly, the results follow a power law of the form $\alpha \sim \phi^{-\epsilon}$, as predicted by Eq. (3). The exponent of this power law is effectively a measure of how important the smaller scales are in the fractal structure; the steeper the curve, the greater resistance the small scales provide.

Similar results were obtained for 15 2D Sierpinski carpets and ten 3D Menger sponges. For each different fractal the values of D_f and D_w for the fluid were found using the box-counting [19] and exact enumeration techniques [20], respectively. The predicted value of the exponent was calculated using Eq. (3) and is compared with the numerically obtained exponent in Fig. 2.

It is clear that the scaling of tortuosity with filling fraction cannot simply be a function of the box-counting dimension, as previously predicted. For example, the theory of [10] only gives a range of predicted ϵ from 0.71 to 0.77. The results show there are fractals with the same value of D_f which have considerably different scaling exponents. The predicted values of ϵ show the right trend when compared to the numerically calculated values of the exponent, although, on the whole, the predicted values overestimate the observed values. We currently have no explanation for this overestimation. The largest discrepancies between the predicted and numerical exponents clearly occur for the 2D case. This can be explained by the ease with which the flow can be blocked in two dimensions, when compared to three dimensions. If the direction of flow is largely obstructed by a part of the porous material, this effect is not taken into account by measuring D_w, which is isotropic. Supporting this idea is the fact that

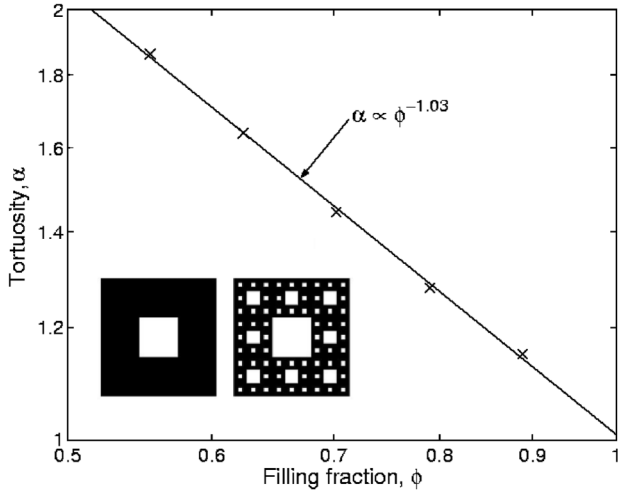

FIG. 1. Variation of tortuosity with filling fraction for a saturated 2D Sierpinski carpet with $D_f = 1.87$ and $D_w = 2.13$. The inset in the bottom left hand corner shows generations 1 and 3 of a Sierpinski gasket.

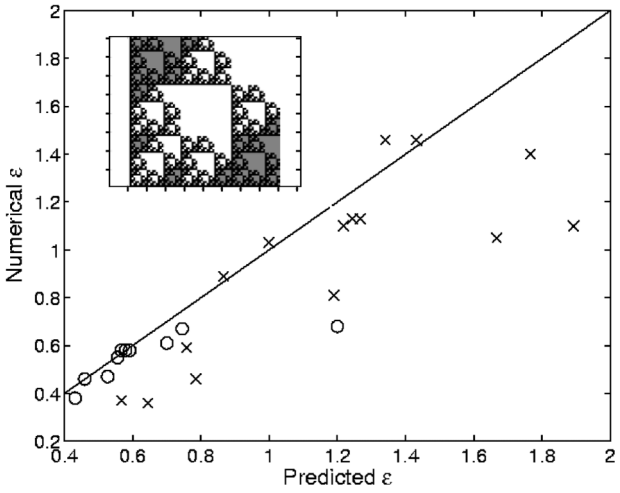

FIG. 2. Comparison of the numerically observed and predicted exponents for 15 2D Sierpinski carpets (×) and ten 3D Menger sponges (○). The straight line predicted ϵ = Numerical ϵ guides the eye. The inset shows generation 4 of the 2D fractal having the largest discrepancy between predicted and numerical exponents.

the area of the bounding box which contains the largest connected cluster of the fractal, which is a measure of the blockage, shows a strong correlation with the magnitude of the discrepancy between the numerical and predicted exponents. The inset of Fig. 2 shows generation 4 of the 2D Sierpinski carpet which exhibited the largest discrepancy between the predicted and numerical exponents. Black shading indicates the ''pores'' of the material. The largest connected cluster, shaded in white (the remaining material is shaded gray), clearly blocks the direction of flow, which is left to right.

The agreement for the 3D Menger sponges is certainly better than for the 2D Sierpinski carpets as it is much harder in three dimensions to generate such a blockage. The only 3D fractal showing a large discrepancy between the predicted and numerical exponents has a porosity $\mathcal{P} = 0.52$ at generation number 4, whereas all the other fractals have $\mathcal{P} > 0.7$ at the same generation number.

The above model provides no way of analyzing stochastic fractals [17], where there is no equivalent of a generator or motif, which is iterated a certain number of times to give the desired level of detail. An alternative way of defractalizing is to adsorb an increasing amount of fluid onto a fractal substrate and to calculate the tortuosity of these films.

Reference [21] describes a method for calculating the adsorption of a fluid onto any lattice based object by means of writing the Hamiltonian of a simple lattice-gas model in the presence of geometrical disorder. Only the energies due to fluid-fluid interaction and solid-fluid interaction, of strengths w_{ff} and w_{sf}, respectively, between nearest neighbors on the lattice are considered. The Hamiltonian is $H = -w_{\mathrm{ff}} \sum_{i<j}^{\mathrm{nn}} \tau_i \tau_j \eta_i \eta_j - w_{\mathrm{sf}} \sum_{i<j}^{\mathrm{nn}} [\tau_i \eta_i (1 - \eta_j) + \tau_j \eta_j (1 - \eta_i)]$, where the sums run over nearest neighbor sites. τ_i is a fluid occupation variable, which indicates whether site i of the lattice is occupied by fluid ($\tau_i = 1$) or not ($\tau_i = 0$). η_i is a quenched variable that characterizes the presence of solid particles at site i ($\eta_i = 0$ if solid is present and $\eta_i = 1$ if not). This method was chosen as it allows the geometrical disorder (pore size and pore connectivity) crucial to this problem to be considered from the outset, as opposed to assuming a pore shape and then using a curve fitting procedure to determine the connectivity of the network. The η_i sets are generated from both diffusion-limited aggregation (DLA) clusters [22] and deterministic fractals in two and three dimensions. The Hamiltonian is treated in the mean-field limit and this leads to a set of coupled nonlinear equations for the fluid density, $\rho_i = \langle \tau_i \eta_i \rangle$, at the lattice sites, where $\langle\rangle$ denotes an average occupancy. Lattice sites i with $\rho_i > 0.5$ are taken to contain fluid, whereas sites i with $\rho_i < 0.5$ are taken as vacant. An example of the adsorption process for a DLA cluster can be seen in fig. 4 of [23]. The calculation of the tortuosity consists of the solution of the potential flow problem described in the saturated case, using the linear finite element scheme. The geometry is defined by the presence of fluid sites from the lattice-gas model.

Figure 3 shows the results for both 2D and 3D deterministic and DLA fractals and it is clear that all of the data are fitted by a power law of the form $\alpha \sim \phi^{-\epsilon}$.

The exponent for the 3D DLA cluster ($\epsilon = 1.04$) is very close to the experimentally measured exponent of $\epsilon = 1.16$ reported for aerogel in [9], which is encouraging as DLA clusters have been proposed as a potential structure for aerogel. One would expect any fractal characteristics of the fluid flow to be lost at higher filling fractions, when the fractal nature of the adsorbed fluid is lost. It is, however, difficult to be conclusive about how far the power law extends to high filling fractions from the numerical data

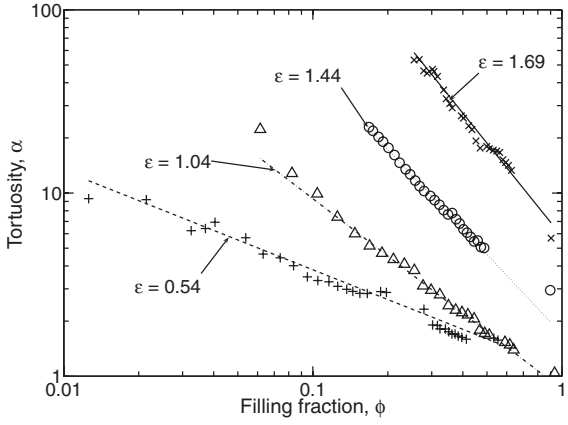

FIG. 3. The numerically calculated tortuosity against filling fraction in the unsaturated model on log-log scale, along with the fitted power laws. (×-) 2D Sierpinski carpet, (○···) 2D DLA cluster, (△.-) 3D DLA cluster, (+-) 3D DLA cluster.

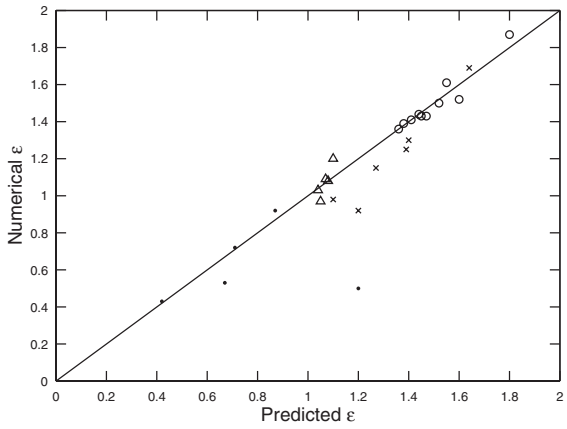

FIG. 4. Comparison of the numerically observed and predicted exponents for the unsaturated model. (×) 2D deterministic fractals, (○) 2D DLA clusters, (.) 3D deterministic fractals, (△) 3D DLA clusters. The straight line predicted $\epsilon =$ Numerical ϵ again guides the eye.

obtained, due to the intrinsic numerical difficulty of obtaining sufficient data at high filling fractions.

Figure 4 shows the values of D_f and D_w calculated for the adsorbed fluid and the numerical scaling exponent compared with the scaling exponent predicted by Eq. (3).

The agreement between the predicted and numerical exponents is generally good, especially for the DLA clusters, where the prediction is even sensitive to small changes in the numerical exponent of different DLA clusters. This suggests that the method is capable of determining the different microstructure of different realisations of the same family of stochastic fractals. The agreement of the numerical and predicted exponents for the deterministic fractals is less impressive, although still good, with the exception of one 3D Menger sponge. Because of the limited number of deterministic fractals considered, it is difficult to say whether the predictions are more accurate for the 2D or 3D cases, but it appears that the agreement in three dimensions is better, as in the saturated case. This observation, in tandem with the better agreement for the stochastic fractals, suggests that the predicted exponent is more accurate for highly porous materials. Again the predicted exponent seems to be an overestimate and this requires further investigation.

In conclusion, tortuosity, an important mesoscopic property in the calculation of the transport properties of porous materials, has been shown to scale with the volume filling fraction of fluid in the material with an exponent that is predominantly a function of the box-counting and random walk dimensions of the fluid. This exponent is not only sensitive to different classes of fractals, i.e., stochastic and deterministic, but also distinguishes between the different structure of stochastic fractals of the same type. The exponent ϵ is an important characteristic as it measures the impact of different length scales on the tortuosity of the material and is a measure of the multiscale nature of materials, which can be accessed experimentally. Further work is needed to understand why the predicted exponent is always an overestimate and what other fractal characteristics may be needed to more accurately predict ϵ.

The authors are grateful to A. I. Golov, S. Babuin, and C. Ashton for many fruitful discussions. Both authors would like to acknowledge support under EPSRC Grant No. GR/S27559/01.

*stuart.coleman@imperial.ac.uk

[1] D. Schaefer and K. Keefer, Phys. Rev. Lett. **56**, 2199 (1986).
[2] A. Katz and A. Thompson, Phys. Rev. Lett. **54**, 1325 (1985).
[3] M. Sahimi, Rev. Mod. Phys. **65**, 1393 (1993).
[4] X. Zhang, M. Knackstedt, and M. Sahimi, Physica (Amsterdam) **233A**, 835 (1996).
[5] P. Spanne, J. F. Thovert, C. J. Jacquin, W. B. Lindquist, K. W. Jones, and P. M. Adler, Phys. Rev. Lett. **73**, 2001 (1994).
[6] R. I. Al-Raoush and C. S. Willson, J. Hydrology **300**, 44 (2005).
[7] A. E. Scheidegger, *The Physics of Flow through Porous Media* (University of Toronto, Toronto, 1974).
[8] D. Johnson, J. Koplik, and R. Dashen, J. Fluid Mech. **176**, 379 (1987).
[9] A. Golov, I. Berkutov, S. Babuin, and D. Cousins, Physica (Amsterdam) **329–333B**, 258 (2003).
[10] P. de Gennes, in *Physics of Disordered Materials*, edited by D. Adler, H. Fritzsche, and S. Ovshinsky (Plenum, New York, 1985), p. 227.
[11] P. Sen, C. Scala, and M. Cohen, Geophysics **46**, 781 (1981).
[12] S. Cohen, R. Guyer, and J. Machta, Phys. Rev. B **34**, 6522 (1986).
[13] S. Havlin and D. Ben-Avraham, Adv. Phys. **36**, 695 (1987).
[14] L. Rayleigh, Philos. Mag. **34**, 481 (1892).
[15] A. Einstein, Ann. Phys. (Leipzig) **322**, 549 (1905).
[16] Y. Gefen and I. Goldhirsch, Phys. Rev. B **35**, 8639 (1987).
[17] H. Peitgen, H. Jurgens, and D. Saupe, *Chaos and Fractals: New Frontiers of Science* (Springer-Verlag, New York, 1992).
[18] O. C. Zienkiewicz and K. Morgan, *Finite Elements and Approximation* (Wiley Interscience Publ., New York, 1983).
[19] J. C. Vassilicos and J. G. Brasseur, Phys. Rev. E **54**, 467 (1996).
[20] I. Majid, D. Ben-Avraham, S. Havlin, and H. E. Stanley, Phys. Rev. B **30**, 1626 (1984).
[21] F. Detcheverry, E. Kierlik, M. Rosinberg, and G. Tarjus, Langmuir **20**, 8006 (2004).
[22] T. A. Witten and L. M. Sander, Phys. Rev. Lett. **47** 1400 (1981).
[23] S. W. Coleman and J. C. Vassilicos, http://www3.imperial.ac.uk/pls/portallive/docs/1/29577697.PDF (2007).